MARS MISSIONS USING SOLAR ELECTRIC PROPULSION

Steven N. Williams[1] and Victoria Coverstone-Carroll[2]

ABSTRACT

Solar Electric Propulsion (SEP) trajectories are shown for Mars missions between late 2004 and 2011. Mission performance is presented as burn-out mass along contours of constant flight time. These missions are characterized by low injection energies, and therefore with a given launch vehicle, greater injected mass. The superior specific impulse of the SEP results in a larger delivered mass at Mars than a conventional chemical mission. It is suggested that Mars sample return missions now being studied may benefit significantly by using SEP. A very curious feature of these missions is that for longer flight times, solutions exist which permit a near continuous launch opportunity over an entire Earth-Mars synodic period.

INTRODUCTION

The possibility of discovering life elsewhere in the solar system has intrigued people for many decades. The announcement that evidence of life may have been found inside Martian meteorites has drawn further attention to this question. NASA is currently studying the possibility of retrieving several samples from the surface of Mars between 2005 and 2011. Without a doubt these will be the most ambitious planetary missions ever undertaken. One must deliver to Mars orbit a flight system which can descend to the surface, retrieve a soil sample, launch this sample back into Mars orbit where it must rendezvous and mate with an Earth return vehicle, and then return it to Earth. There will be many challenging aspects to these missions, not the least of which will be overcoming the large mass performance requirements on a streamlined budget.

We wish to show that there is potentially a significant performance advantage to using SEP for Mars missions. We examine only the interplanetary phase of the mission. We do not consider Mars orbit insertion, nor try to compare the various strategies one might use: chemical, aerobraking, aerocapture, SEP, or some combination of these. Also, the reader should recognize that the dry mass of a SEP system will be greater than that of a chemical system. This will consume some of the performance advantage shown below. Nevertheless, this performance advantage will be somewhere between 150 and 900 kg - depending on how one does the comparison, so this should be sufficient to justify a serious examination of SEP.

We have previously compared SEP and chemical performance for several different planetary missions [1]. We believe a Mars sample return is an excellent example of the type of mission where SEP should be superior to conventional missions: a large "interplanetary ΔV" requirement on a mission which stays in the inner solar system. SEP is currently being tested on NASA's Deep Space 1 mission (DS1) [2]. The successful demonstration of SEP on this mission should pave the way for its use on missions like the ones described in this paper.

---

[1] Senior Engineer, Navigation & Flight Mechanics Section, Jet Propulsion Laboratory, California Institute of Technology, Pasadena, CA 91109.

[2] Associate Professor, Department of Aeronautical & Astronautical Engineering, University of Illinois at Urbana-Champaign, Urbana, IL 61801.

In addition to Mars sample return missions, we also consider a less ambitious Mars orbiter mission. The interplanetary trajectories are computed in the same way. However, for the orbiter mission we assume a smaller launch vehicle and a simpler flight system. We show here that as the flight time is increased, the launch period gets broader. At some point, we observe the rather curious fact that one can actually launch any day of the year with only moderate changes in mass performance. This behavior was initially discovered while examining a new technique (a hybrid genetic algorithm and calculus-of-variations approach) for low thrust trajectory optimization [3],[4].

MODELS

The SEP trajectories reported in this paper were optimized with Solar Electric Propulsion Trajectory Optimization Program (SEPTOP). SEPTOP is a modification of the Variable Thrust Trajectory Optimization Program (VARITOP) [5]. SEPTOP models the SEP throttling characteristics as a function of available solar array power. It uses a traditional calculus-of-variations approach. SEPTOP computes an optimum trajectory such that the burnout mass is maximized by varying the thrust profile and launch energy ($C_3 = V_p^2 - 2\,\mu/R_p$, where V_p and R_p are Earth periapsis velocity and radius and μ is the product of the universal gravitational constant and mass of Earth). Injected mass at Earth was determined from a launch vehicle performance curve (holding a 5% contingency). A Delta II class launch vehicle (1300 kg injected mass to a C_3 of 0) was assumed for the "orbiter missions", and a Delta III class launch vehicle (2720 kg injected mass to a C_3 of 0) for the "sample return missions". As mentioned above, no Mars orbit insertion strategy is considered. All SEP trajectories reported here rendezvous (match position and velocity) with Mars - that is, they arrive with a hyperbolic excess velocity (V_∞) of zero. A two-body gravitation model is used.

For SEP, the key spacecraft parameters are thruster performance and solar array power. We assume NSTAR (NASA Solar Electric Propulsion Technology Applications Readiness Program) thrusters [6]. A polynomial approximation to thrust and mass flow rate was used:

$$\text{mass flow rate (milligram/s)} = 0.74343 + .20951P + .25205P^2$$
$$\text{thrust (millinewtons)} = -3.4318 + 37.365P$$

where P is the power processing unit input (PPU) power in kilowatts. Maximum input power to each PPU is 2.53 kW. Performance curves for the solar array were reported in Ref. [1]. SEP thrust and mass flow rate were reduced to 90% of their nominal value (referred to here as duty cycle) to provide additional margin, and also account for time to perform optical navigation and other spacecraft functions incompatible with simultaneously operating the thrusters. For the orbiter missions, one thruster and a 5 kW array were used. For the sample return trajectories, two thrusters with 8 and 10 kW arrays were considered. In all cases 400 W of power were allocated to operate spacecraft systems and not therefore available to the propulsion system.

Most of the results presented were found by performing parametric studies with SEPTOP. This involved following each of the contours shown (constant flight time) in the figures below by incrementing the launch date, and reoptimizing the trajectory. The algorithm involved makes use of gradient information, and in general works very well. Sometimes, when a fundamentally different solution becomes more optimum, the software has problems making the transition between the two. Frequently this implies a different sequence of thrust and coast phases.

We have been experimenting with methods that do not rely entirely on gradients. One such successful experimentation coupled a multi-objective genetic algorithm with SEPTOP in hopes that by using the genetic algorithm's strength of evolving multiple solutions, a large percentage of the search space could be sampled and different classes of trajectories might be identified. The genetic algorithm was used to identify the initial values for the independent variables required to execute SEPTOP. This hybrid algorithm (genetic algorithm + SEPTOP) is described in detail in Ref. [3] and [4]. The hybrid algorithm was applied to both the sample return and orbiter missions. In addition to identifying different "classes" of solutions, this technique also generates a set of trajectories within each class with similar characteristics - not unlike the parametric data generated with SEPTOP that will be discussed in this paper. As stated above, we did find a unique class of solutions using the hybrid algorithm, one of which is shown in Fig. 1. This particular solution consists of a series of 4 coast and 4 burn arcs - and would generally be quite challenging to find using software such as SEPTOP as a stand-alone optimizer. In fact, having found this solution with the hybrid software, we tried unsuccessfully to transition between it and the other solutions we found using the parametric techniques described above.

SAMPLE RETURN MISSIONS

We computed trajectories to Mars for launch dates between the middle of 2004 and late 2009 - slightly less than three Earth-Mars synodic periods. The results are shown in Figures 2a and 2b. We show contours of constant flight time between 1.5 and 3.0 years. This time span covers three distinct sets of opportunities. We used a 10 kW solar array to power two NSTAR thrusters. In Fig. 2b, we also show the effect of less power (8 kW) during the first opportunity. All the trajectories in these figures arrive at Mars with a V_∞ of 0.0. In practice, the method used for Mars orbit insertion might be chemical, SEP, or some form of aerocapture, but as previously mentioned this phase of the mission is not modeled. We also point out that SEP can be used to arrive with any desired V_∞. Fig. 3 shows the performance impact of arriving at different velocities on a two year mission launched in July 2005 (from Fig. 2b).

For comparison purposes, we indicate the location of each ballistic or chemical opportunity with a vertical dashed line. We also provide performance results in Table 1 for several chemical orbit insertion strategies. The aerocapture cases simulate a situation where no propulsive energy is required for Mars orbit insertion. Comparing the "Burnout Mass" column in Table 1 to Figs. 2, one immediately sees that the SEP will almost certainly outperform any strategy which relies on a propulsive Mars capture. Nevertheless, the results presented here do not allow one to make a direct comparison, both because the SEP trajectories shown do not achieve a Mars capture orbit, and because the difference between SEP and chemical propulsion system masses is not provided. Also, in addition to a full SEP scenario, one might want to examine SEP with an aerocapture strategy at Mars. We show in Fig. 3 that the SEP can be used to achieve "any" desired approach velocity. Nevertheless, the purpose of this paper is not to suggest that SEP is clearly the best option, since many necessary trades remain to be done. We do believe however, the results shown here indicate that SEP may provide a significant performance benefit for Mars missions, and that further examination of this approach is warranted.

Figures 2a and 2b display the SEP results used to analyze the Earth to Mars portion of the sample return mission. The performance of the shorter flight time trajectories displays a familiar behavior with a single maximum, tapering off rapidly in a symmetrical manner as you move away from the optimum launch date. However, as the flight time is increased, one observes a rather peculiar behavior. A second maximum appears with an

earlier launch date. At first, there are two maxima which are not continuously connected, but further increases in the flight time results in a continuous set of solutions between the two maxima. At longer flight times, the later maxima transitions into an "inflection point" and eventually disappears, so that only the earlier one is present. Finally, if one goes to a long enough flight time (4.67 years here), there are continuous solutions across the entire 5 1/2 years shown in the plot.

As mentioned earlier, we could not transition between the two types of solutions (4.67 and 3.5 yr.) using SEPTOP alone. The solutions are too different for a gradient technique to "bridge the gap". In this case, the long flight time will make the result impractical for Mars mission design purposes, but can be important in understanding the sometimes non-intuitive nature of low thrust trajectories. It also illustrates the fact that the traditional pure gradient based methods for doing interplanetary trajectory optimization are fine for doing parametric studies over a region where only moderate changes are expected to occur. However, they will be inadequate when searching for SEP trajectories on many missions where a more complicated interplanetary trajectory (multiple heliocentric revolutions or multiple gravity-assist encounters or both) is required.

One might expect the best performance to correlate with arriving at Mars at a node (as with ballistic trajectories) so that the SEP does not have to thrust out of the ecliptic plane, or to arrive near perihelion where the power and therefore available thrust are the greatest. These points are shown on the curves in Figs. 2a and 2b. Interestingly, for the 1.5 year flight times, the optimum solution results in a compromise which falls between these points. As one goes to longer flight times, the correlation is better. Both the two and three year flight times want to arrive near the ascending node. The 2.5 year curves are more like the 1.5 year curves, with the peak performance falling between these points.

It is also instructive to examine the change in the trajectory at selected points in Fig. 2b. The trajectories in Fig. 4 correspond to the letters A - F in Fig. 2b. Additional information on these trajectories is shown in Table 2. The letters C - F are all on the 2.5 year contour in Fig 2b. The solutions at A and B represent other points of interest. The solution at A is the shortest flight time (1.4 year) in this family of solutions which can be flown (subject to the other constraints in the problem: launch vehicle performance curve, solar array, duty cycle, ...). It requires continuous unbroken thrusting from launch to Mars arrival. The trajectory at point B represents the peak performance on the 2 year curve, and contains one coast arc. Point C represents a local optimum on the 2.5 year curve. Here the optimum solution now has a second coast arc. Point D represents a slight dip in the performance where the two coast arcs have shifted somewhat. At point E, the second coast arc has disappeared leaving only one coast arc again. Finally at point F, which has the greater performance of the two optima, a second coast arc has appeared early in the mission. Point F is also unique in one other aspect. The others reach solar ranges near Mars very early in the mission. They then either "fall back in" or use the SEP to rendezvous with Mars as quickly as possible. The point F trajectory has a more continuous spiral out to Mars, doing more of its thrusting well inside Mars' orbit where the SEP is more efficient. This results in better mass performance.

Consistent with the discussion above, one can see in Table 2 that increased performance (burnout mass) corresponds to decreasing launch energy. This is not too surprising, since it means more of the mission ΔV is being imparted with the more efficient SEP than with the launch vehicle upper stage. In this example, the increased performance also correlates with larger heliocentric revs. The best performance occurs when the planetary geometry is such that the transfer angle is greatest. This permits a lower C_3 (and therefore larger injected mass) and a "tighter spiral" which means more time is spent close to the sun where the SEP is more efficient.

Figure 5 shows similar plots for Earth return trajectories. These trajectories all begin at Mars with a V_∞ of zero and an initial mass of 700 kg. As in Figs. 2, there is also some indication of double maxima in these plots, though it varies somewhat from year to year. There is no evidence that a longer return time translates into better performance - just a broader opportunity. Also, the 10 kW array provides very little advantage over the 8 kW array for the return leg. The choice of 700 kg was somewhat arbitrary. A more realistic value would require a more detailed mass estimate for the spacecraft and Earth re-entry vehicle, but this is probably a reasonable first approximation. As a point of reference, the DS1 inert spacecraft mass (including everything but Xenon) with only one thruster and a 2.5 kW array was about 400 kg.

Figure 6 illustrates how the trajectory changes for four points from Fig. 5. Point A represents the maximum performance on the one year curve. It has a fairly simple profile with a burn arc followed by a coast arc. As the flight time is increased between A and B, the departure date moves earlier, but the beginning of the thrust arc stays about the same (to within a week). For all practical purposes, A and B are the same trajectory. These trajectories arrive back at Earth with a V_∞ of about 2.65 km/s. Points C and D are local maxima on the 2 year curve. Between B and C, an early thrust arc has appeared, and the original thrust arc has shortened in duration. Both are about 3 months long. The Earth V_∞ has also gone up. Though the effect is small here, similar to trajectory F in Fig. 4, note that C does a larger fraction of its thrusting closer to the sun (where the SEP is more efficient) than the other three, and also has the better mass performance. In D the earlier thrust arc has increased in duration while the later one has shortened. It has slightly less mass performance than C.

ORBITER MISSIONS

Trajectories to Mars for launch dates between the middle of 2004 and late 2009 were computed. The results are shown in Fig 7. This time span covers three distinct sets of opportunities. We show contours of constant flight time between 1.5 and 3.5 years. For these trajectories, we used a Delta II class launch vehicle, and a 5 kW solar array to power the SEP. As in Figs. 2, these trajectories arrive at Mars with $V_\infty = 0$. In the 2005 opportunity we see behavior very similar to that in Fig. 2a with double maxima. The other two opportunities show some evidence of the double maxima, but really look more like the profiles in Fig. 5 where longer flight times give broader launch opportunities, but not much performance advantage. As before, we indicate the location of each ballistic or chemical opportunity with a vertical dashed line. Using the genetic algorithm code described earlier, we found a 3.5 year contour to be continuous across the range of launch dates examined.

CONCLUSIONS

We believe there are two important conclusions to be drawn from this analysis. The first is that SEP has the potential to offer significant performance advantage to Mars sample return missions currently being studied. This is precisely the type of mission where SEP should compare favorably with chemical propulsion systems. The Mars rendezvous and departure require a large interplanetary ΔV, and the mission remains in the inner solar system where solar power is available to drive the SEP. We showed that for short flight times, SEP performance curves have a symmetric profile similar to ballistic trajectories. As the flight time increases, the trajectories become more complicated with a series of "burn - coast" arcs which result in somewhat non-intuitive behavior. We also showed that using SEP allows one to both significantly reduce and also vary the arrival velocity - reducing the thermal load on an aerobrake or aerocapture mission if one were combined with the SEP.

The second conclusion is that in designing interplanetary SEP missions, we are limited when using only traditional gradient-based optimization techniques. It would have been very difficult, if not impossible to find the trajectories which exhibited the continuous launch opportunities using only the gradient-based software. The point is that for relatively simple (or moderately difficult) trajectories these traditional techniques work fine. If we ever want to fly SEP versions of multiple gravity-assist trajectories such as Galileo or Cassini, we will almost certainly have to incorporate non gradient-based techniques such as genetic algorithms to map the complete solution space.

REFERENCES

[1] Williams, S.N. and Coverstone-Carroll, V. "Benefits of Solar Electric Propulsion for the Next Generation of Planetary Exploration Missions," *Journal of the Astronautical Sciences*, Vol. 45, No. 2, April-June 1997, pp. 143-159.

[2] Rayman, M.D., Chadbourne, P.A., Culwell, J.S. and Williams, S.N. "Mission Design for Deep Space 1: A Low-Thrust Technology Validation Mission," Paper No. IAA-L98-0502, Third IAA International Conference on Low-Cost Planetary Missions, Pasadena, California, April 27 - May 1, 1998.

[3] Hartmann, J.W. , Coverstone-Carroll, V. and Williams, S.N. "Optimal Interplanetary Spacecraft Trajectories Via a Pareto Genetic Algorithm," Paper No. 98-202, AAS/AIAA Space Flight Mechanics Meeting, Monterey, California, February 1998.

[4] Hartmann, J.W. , Coverstone-Carroll, V. and Williams, S.N. "Optimal Interplanetary Spacecraft Trajectories Via a Pareto Genetic Algorithm," *Journal of the Astronautical Sciences*, accepted for publication.

[5] Sauer, C.G. Jr. "Optimization of Multiple Target Electric Propulsion Trajectories", AIAA Paper 73-205, AIAA 11th Aerospace Sciences Meeting, Washington, D.C., January 10-12, 1973.

[6] Sovey, J.S., et.al, "Development of an Ion Thruster and Power Processor for New Millennium's Deep Space 1 Mission," AIAA Paper 97-2778, July 1997; also NASA TM 113129.

FIGURE TITLES

FIG. 1 - LONG FLIGHT TIME MARS TRAJECTORY

FIG. 2a - SEP EARTH to MARS MASS PERFORMANCE (DELTA III)

FIG. 2b - 2005 SEP EARTH to MARS MASS PERFORMANCE

FIG. 3 - SEP MASS PERFORMANCE vs. MARS ARRIVAL V_∞

FIG. 4 - SEP EARTH to MARS HELIOCENTRIC TRAJECTORY PLOTS (2004-2005)

FIG. 5 - SEP MARS to EARTH MASS PERFORMANCE

FIG. 6 - SEP MARS to EARTH HELIOCENTRIC TRAJECTORY PLOTS (2004-2005)

FIG. 7 - SEP EARTH to MARS MASS PERFORMANCE (DELTA II)

TABLE TITLES

TABLE 1 - CHEMICAL MISSION PERFORMANCE CHARACTERISTICS

TABLE 2 - TRAJECTORY CHARACTERISTICS FOR SELECTED MISSIONS

	L/D	C_3 (KM^2/S^2)	TOF (YR)	BURNOUT MASS (KG)[1]	PROPELLANT MASS (KG)
Aerocapture[a]	1 Sep 05 [2]	15.45	1.101	1817	0
	22 Sep 07 [3]	12.75	1.011	1940	0
	14 Oct 09 [4]	10.27	0.897	2056	0
3 day Mars orbit [b]	4 Aug 05	16.65	0.933	1299	465
	11 Sep 07	13.57	0.939	1503	398
	13 Oct 09	10.28	0.887	1636	420
1 day Mars orbit [b]	4 Aug 05	16.65	0.933	1249	515
	11 Sep 07	13.57	0.939	1446	456
	13 Oct 09	10.28	0.887	1573	483
low circular orbit [b]	4 Aug 05	16.65	0.933	869	895
	11 Sep 07	13.57	0.939	1006	896
	13 Oct 09	10.28	0.887	1094	962

(1) Delta III class launch vehicle , Isp = 320 sec
Mars Arrival V_∞ (km/s) : (2) 3.51 (3) 2.83 (4) 2.47
(a) launch/arrival dates optimized to minimize C_3 (arrival periapsis radius = 3900 km)
(b) launch/arrival dates optimized to minimize C_3 + arrival ΔV (arrival periapsis radius = 3900 km)

Table 1

TRAJ TYPE	L/D	C_3 / DLA[1]	BURNOUT MASS (KG)	PROPELLANT MASS (KG)	THRUST SEQUENCE[2]	HELIOCENTRIC REVS
A	4 Aug 05	9.9 / 7.5	1880	196	b	0.81
B	26 Jul 05	7.9 / 10.7	1939	235	b - c - b	1.18
C	6 Jun 05	6.8 / -10.3	1965	264	b - c - b - c - b	1.52
D	7 May 05	6.0 / -22.5	1964	305	b - c - b - c - b	1.56
E	12 Jan 05	2.9 / 7.6	2056	374	b - c - b	1.69
F	29 Oct 04	1.9 / 28.5	2148	334	b - c - b - c - b	1.77

(1) Declination of Launch Asymptote (2) b - burn or thrust arc , c - coast arc

Table 2

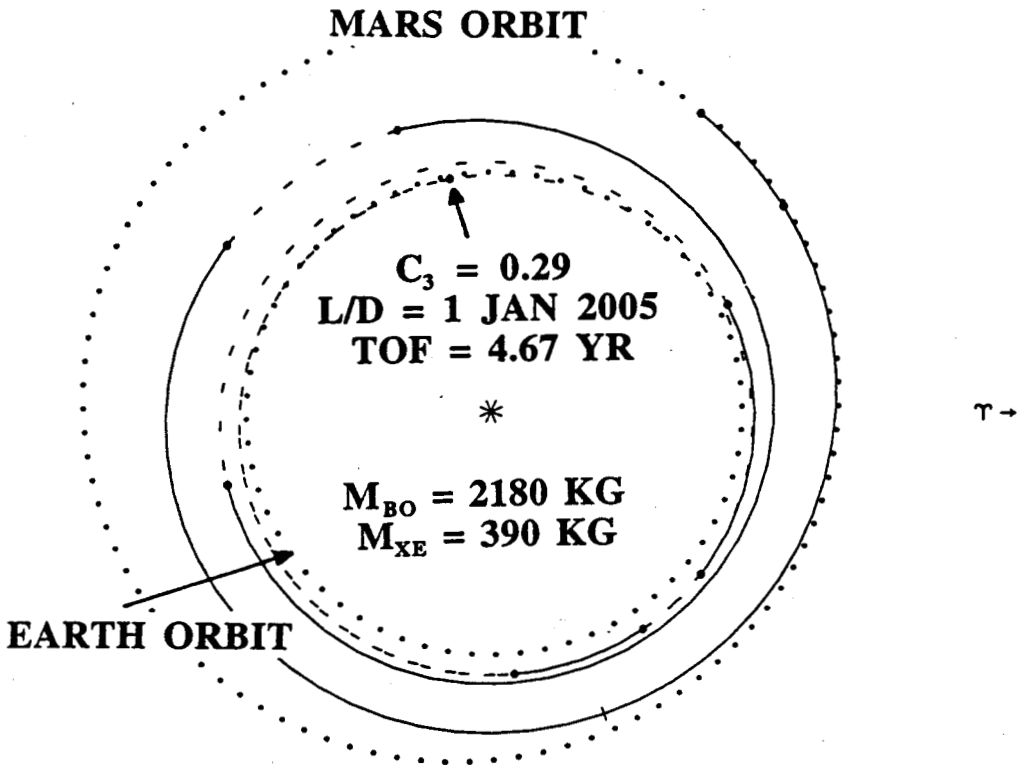
MARS ORBIT
C_3 = 0.29
L/D = 1 JAN 2005
TOF = 4.67 YR
M_{BO} = 2180 KG
M_{XE} = 390 KG
EARTH ORBIT
SOLID LINES : THRUSTING
DASHED LINES : COASTING

Fig 1

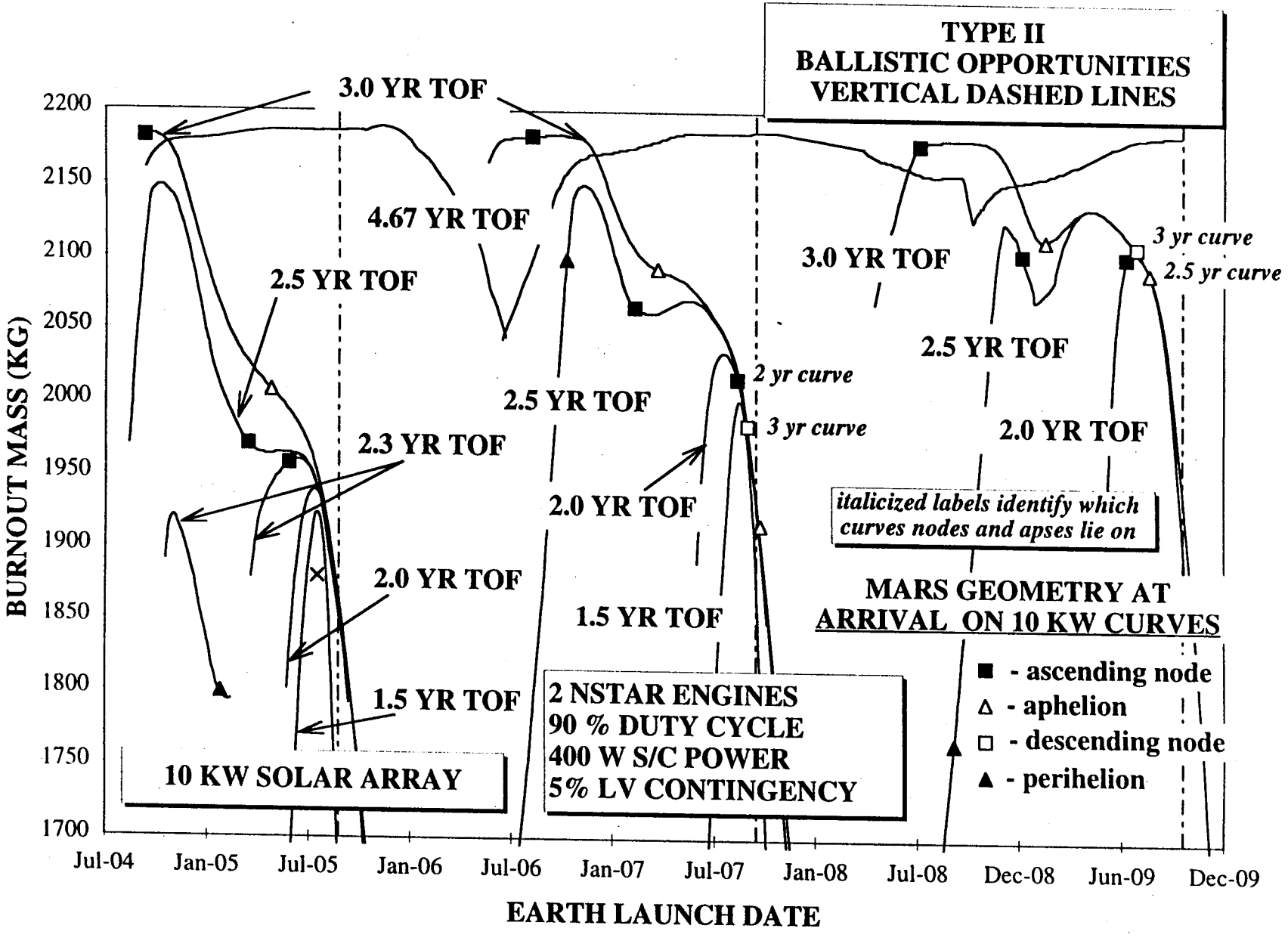
TYPE II
BALLISTIC OPPORTUNITIES
VERTICAL DASHED LINES
3.0 YR TOF
4.67 YR TOF
2.5 YR TOF
2.3 YR TOF
2.0 YR TOF
1.5 YR TOF
3.0 YR TOF
2.5 YR TOF
2.0 YR TOF
1.5 YR TOF
2 yr curve
3 yr curve
2.5 yr curve
3 yr curve
2.5 YR TOF
2.0 YR TOF
italicized labels identify which curves nodes and apses lie on
MARS GEOMETRY AT ARRIVAL ON 10 KW CURVES
■ - ascending node
△ - aphelion
□ - descending node
▲ - perihelion
2 NSTAR ENGINES
90 % DUTY CYCLE
400 W S/C POWER
5% LV CONTINGENCY
10 KW SOLAR ARRAY
BURNOUT MASS (KG)
2200
2150
2100
2050
2000
1950
1900
1850
1800
1750
1700
Jul-04
Jan-05
Jul-05
Jan-06
Jul-06
Jan-07
Jul-07
Jan-08
Jul-08
Dec-08
Jun-09
Dec-09
EARTH LAUNCH DATE

Fig 2a

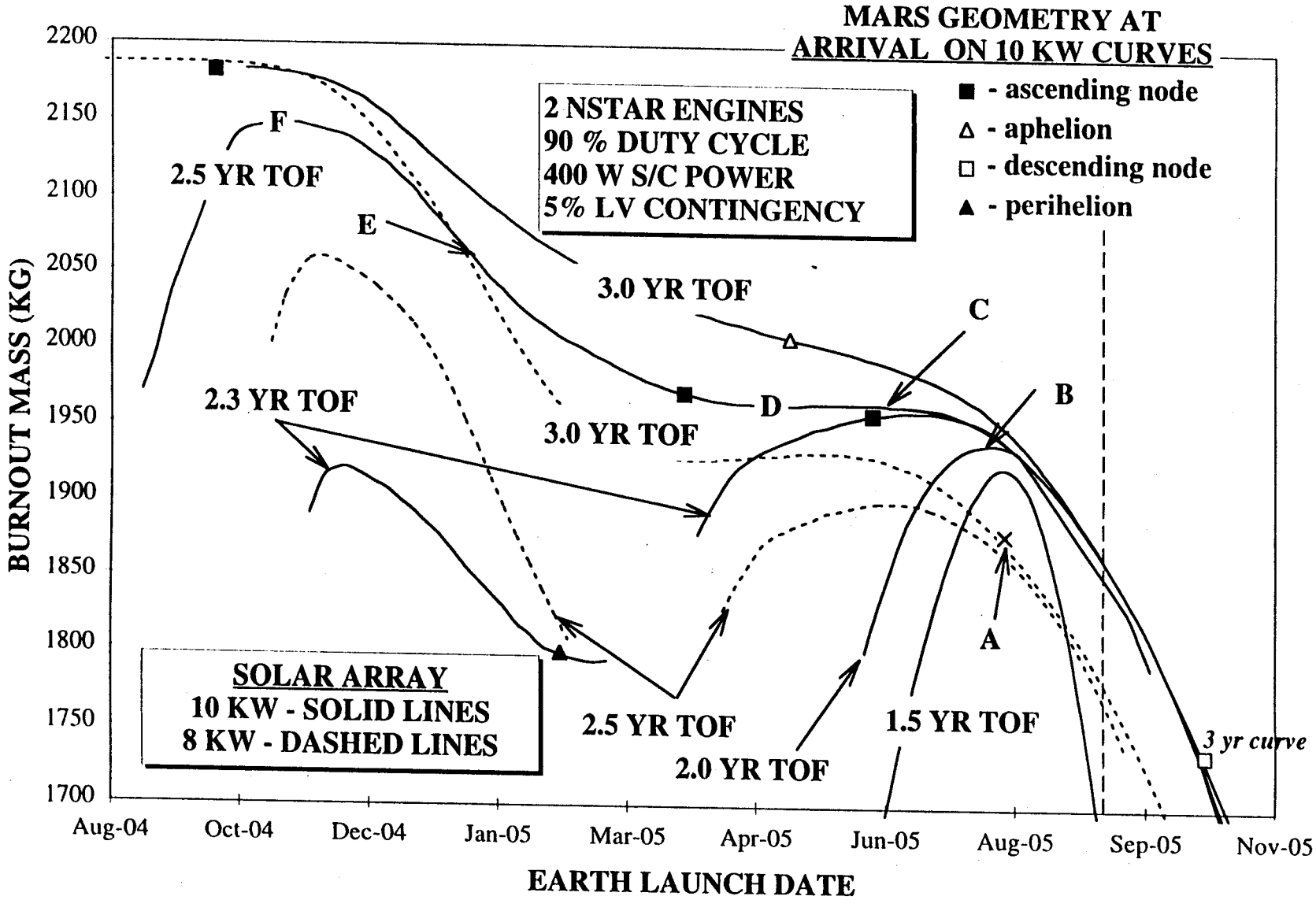
MARS GEOMETRY AT
ARRIVAL ON 10 KW CURVES
■ - ascending node
△ - aphelion
□ - descending node
▲ - perihelion
2 NSTAR ENGINES
90 % DUTY CYCLE
400 W S/C POWER
5% LV CONTINGENCY
SOLAR ARRAY
10 KW - SOLID LINES
8 KW - DASHED LINES
BURNOUT MASS (KG)
2200
2150
2100
2050
2000
1950
1900
1850
1800
1750
1700
Aug-04
Oct-04
Dec-04
Jan-05
Mar-05
Apr-05
Jun-05
Aug-05
Sep-05
Nov-05
EARTH LAUNCH DATE
F
2.5 YR TOF
E
3.0 YR TOF
C
D
B
2.3 YR TOF
3.0 YR TOF
A
2.5 YR TOF
2.0 YR TOF
1.5 YR TOF
3 yr curve

Fig 26

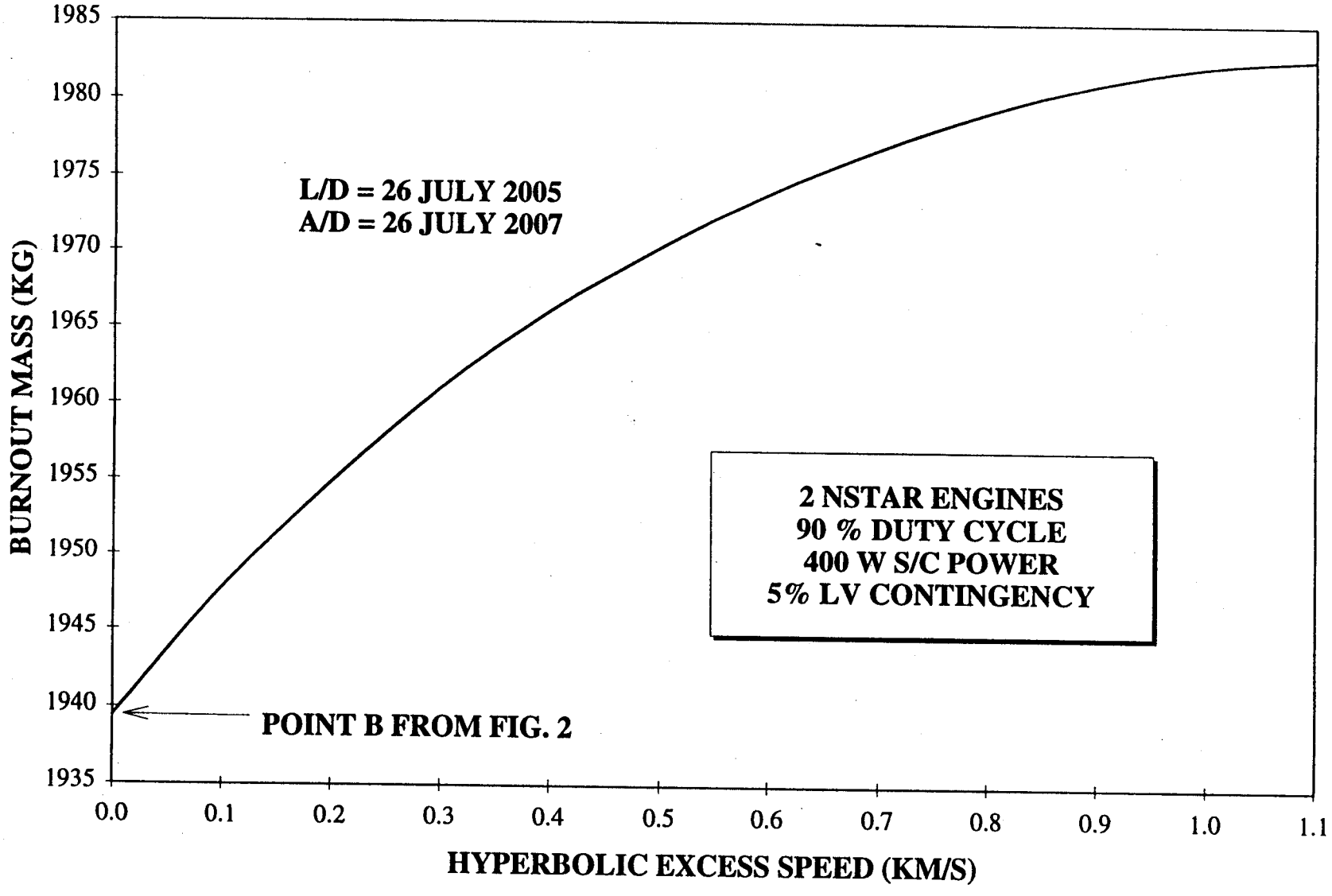
BURNOUT MASS (KG)
1985
1980
1975
1970
1965
1960
1955
1950
1945
1940
1935
L/D = 26 JULY 2005
A/D = 26 JULY 2007
2 NSTAR ENGINES
90 % DUTY CYCLE
400 W S/C POWER
5% LV CONTINGENCY
POINT B FROM FIG. 2
0.0
0.1
0.2
0.3
0.4
0.5
0.6
0.7
0.8
0.9
1.0
1.1
HYPERBOLIC EXCESS SPEED (KM/S)

Fig 3

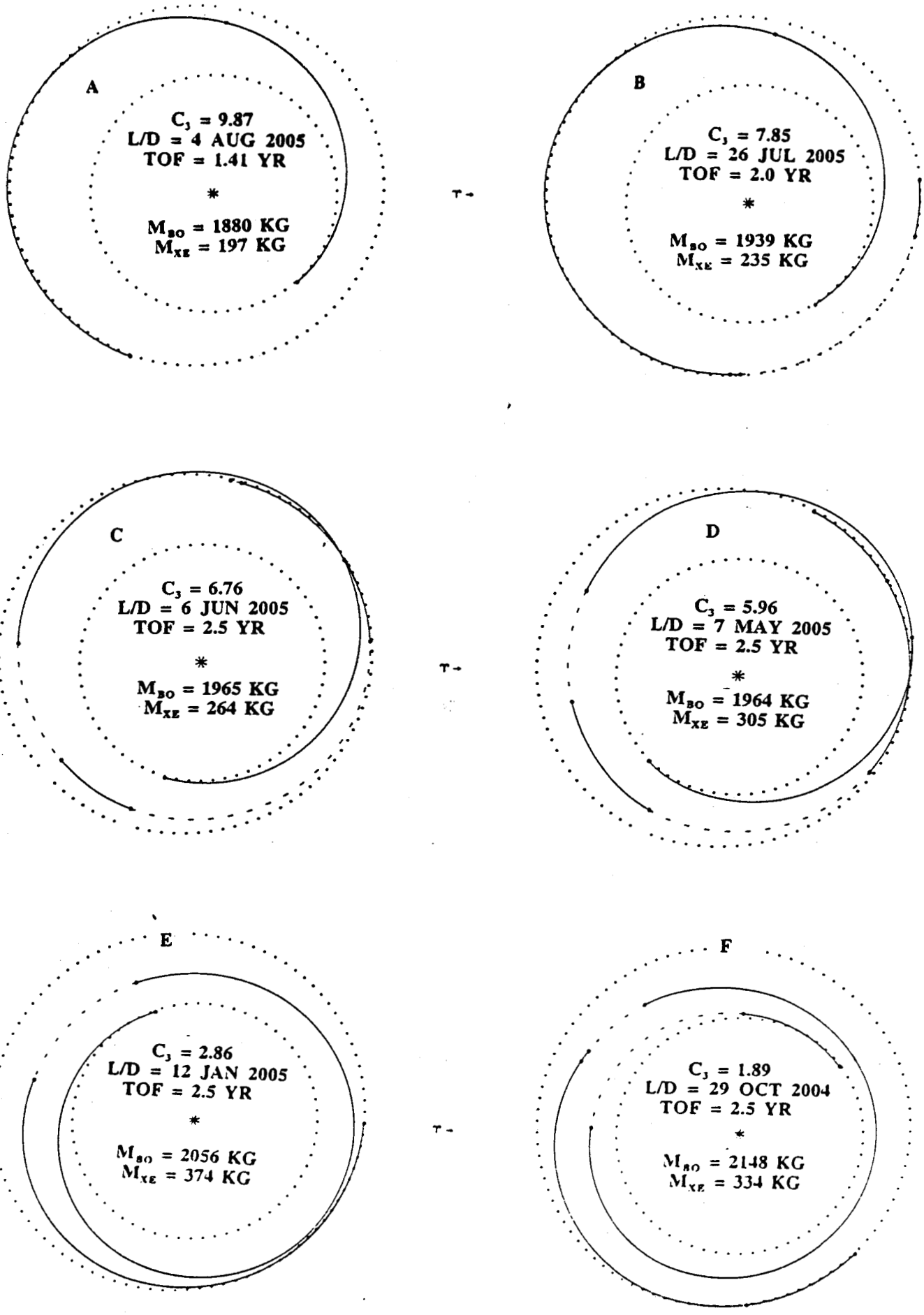
A
C_3 = 9.87
L/D = 4 AUG 2005
TOF = 1.41 YR
M_{BO} = 1880 KG
M_{XE} = 197 KG
B
C_3 = 7.85
L/D = 26 JUL 2005
TOF = 2.0 YR
M_{BO} = 1939 KG
M_{XE} = 235 KG
C
C_3 = 6.76
L/D = 6 JUN 2005
TOF = 2.5 YR
M_{BO} = 1965 KG
M_{XE} = 264 KG
D
C_3 = 5.96
L/D = 7 MAY 2005
TOF = 2.5 YR
M_{BO} = 1964 KG
M_{XE} = 305 KG
E
C_3 = 2.86
L/D = 12 JAN 2005
TOF = 2.5 YR
M_{BO} = 2056 KG
M_{XE} = 374 KG
F
C_3 = 1.89
L/D = 29 OCT 2004
TOF = 2.5 YR
M_{BO} = 2148 KG
M_{XE} = 334 KG

Fig 2

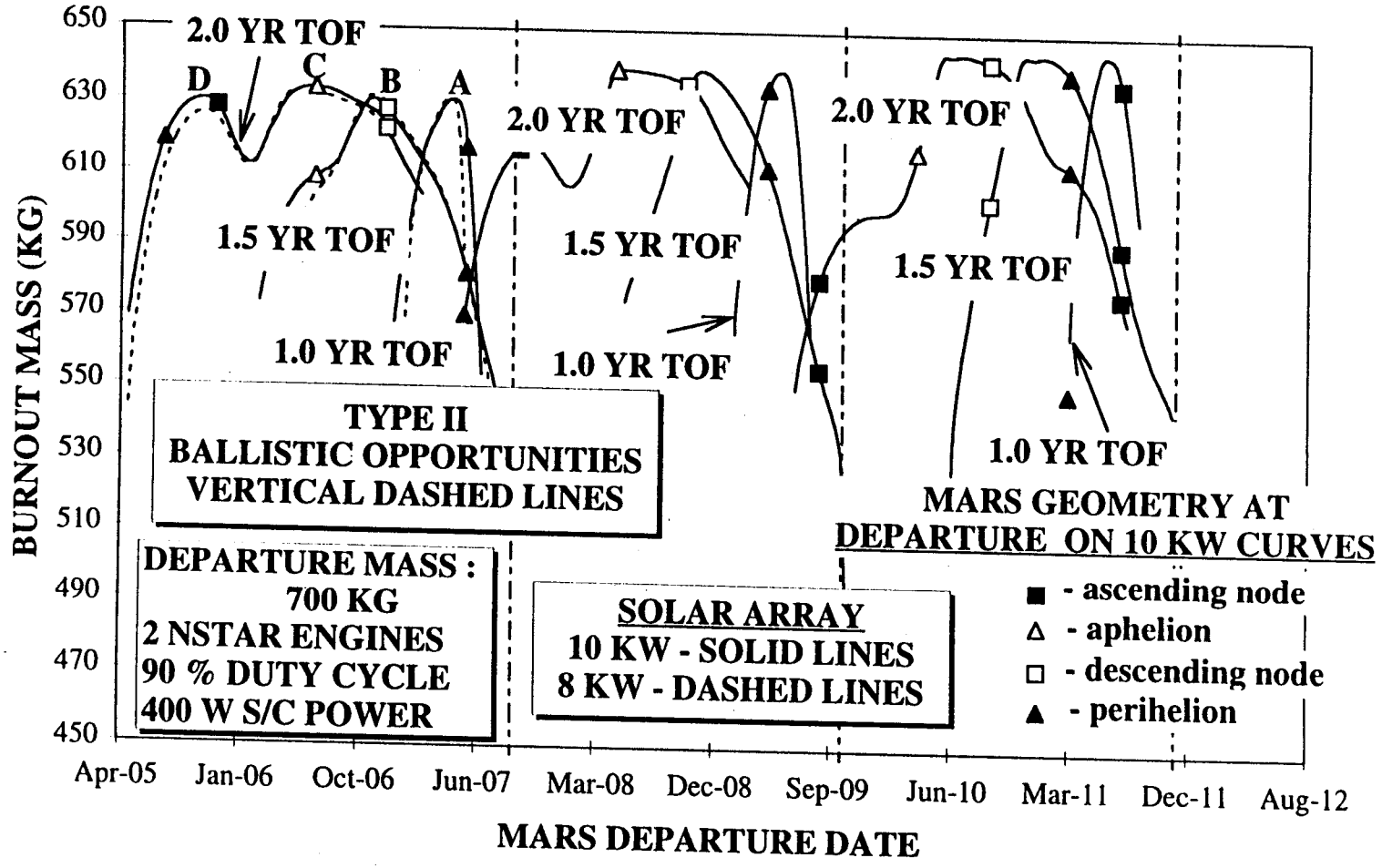
650
630
610
590
570
550
530
510
490
470
450
BURNOUT MASS (KG)
2.0 YR TOF
D
C
B
A
2.0 YR TOF
2.0 YR TOF
1.5 YR TOF
1.5 YR TOF
1.5 YR TOF
1.0 YR TOF
1.0 YR TOF
1.0 YR TOF
TYPE II
BALLISTIC OPPORTUNITIES
VERTICAL DASHED LINES
DEPARTURE MASS :
700 KG
2 NSTAR ENGINES
90 % DUTY CYCLE
400 W S/C POWER
SOLAR ARRAY
10 KW - SOLID LINES
8 KW - DASHED LINES
MARS GEOMETRY AT
DEPARTURE ON 10 KW CURVES
■ - ascending node
△ - aphelion
□ - descending node
▲ - perihelion
Apr-05
Jan-06
Oct-06
Jun-07
Mar-08
Dec-08
Sep-09
Jun-10
Mar-11
Dec-11
Aug-12
MARS DEPARTURE DATE

Fig 5

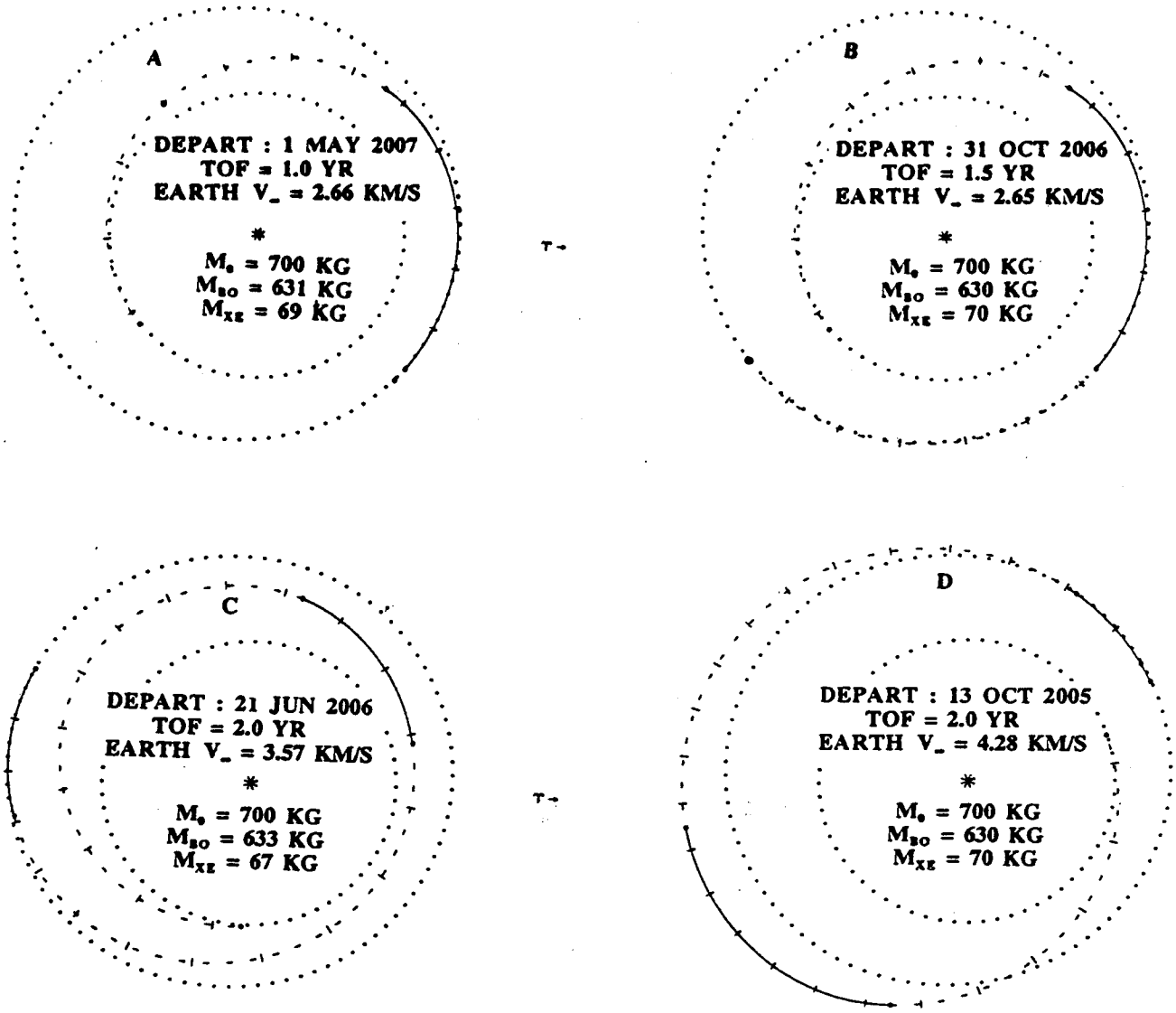
A
DEPART : 1 MAY 2007
TOF = 1.0 YR
EARTH V_ = 2.66 KM/S
*
M₀ = 700 KG
M₈₀ = 631 KG
M_Xe = 69 KG
B
DEPART : 31 OCT 2006
TOF = 1.5 YR
EARTH V_ = 2.65 KM/S
*
M₀ = 700 KG
M₈₀ = 630 KG
M_Xe = 70 KG
C
DEPART : 21 JUN 2006
TOF = 2.0 YR
EARTH V_ = 3.57 KM/S
*
M₀ = 700 KG
M₈₀ = 633 KG
M_Xe = 67 KG
D
DEPART : 13 OCT 2005
TOF = 2.0 YR
EARTH V_ = 4.28 KM/S
*
M₀ = 700 KG
M₈₀ = 630 KG
M_Xe = 70 KG

Fig 6

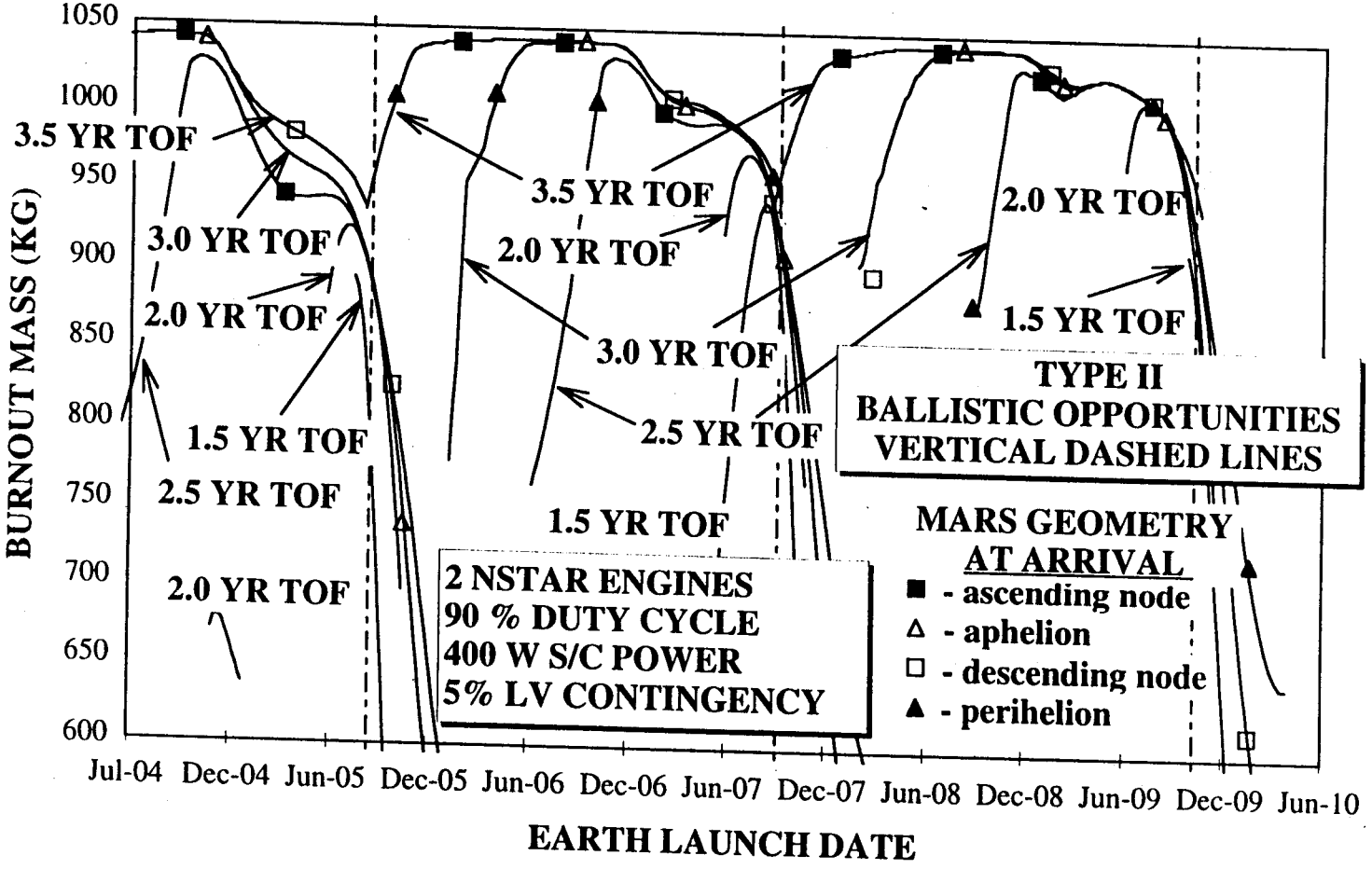
BURNOUT MASS (KG)
1050
1000
950
900
850
800
750
700
650
600
Jul-04
Dec-04
Jun-05
Dec-05
Jun-06
Dec-06
Jun-07
Dec-07
Jun-08
Dec-08
Jun-09
Dec-09
Jun-10
EARTH LAUNCH DATE
3.5 YR TOF
3.0 YR TOF
2.0 YR TOF
1.5 YR TOF
2.5 YR TOF
2.0 YR TOF
3.5 YR TOF
2.0 YR TOF
3.0 YR TOF
2.5 YR TOF
1.5 YR TOF
2.0 YR TOF
1.5 YR TOF
TYPE II
BALLISTIC OPPORTUNITIES
VERTICAL DASHED LINES
2 NSTAR ENGINES
90 % DUTY CYCLE
400 W S/C POWER
5% LV CONTINGENCY
MARS GEOMETRY
AT ARRIVAL
■ - ascending node
△ - aphelion
□ - descending node
▲ - perihelion

Fig 7